

IDENTIFYING REFLECTED GPS SIGNALS AND IMPROVING POSITION ESTIMATION USING 3D MAP SIMULTANEOUSLY BUILT WITH LASER RANGE SCANNER

Ashwani Kumar^{*1}, Yoshihiro Sato^{*2}, Takeshi Oishi^{*3} and Katsushi Ikeuchi^{*4}

^{*}Computer Vision Laboratory, Institute of Industrial Science, The University of Tokyo, Ee-405, 3rd Dept., 4-6-1 Komaba, Meguro-ku, Tokyo, 153-8505, JAPAN. Phone +81-3-5452-6242 Fax +81-3-5452-6244
Email: {akumar¹, yoshi², oishi³, ki⁴}@cvl.iis.u-tokyo.ac.jp

ABSTRACT

In this paper, an operational and viable method to improve GPS position estimation in an urban scenario is presented. The method works by identifying non line of sight satellites w.r.t. a GPS antenna. Subsequently, those signals are excluded from the position estimation calculation. Raw GPS measurements are obtained which give positions of satellites and their pseudo-ranges. A laser range sensor is used to simultaneously build a 3D map of the environment around the measurement point. The satellites are projected on to a rendered 3D scan to find the satellites which are not in the line of sight with the GPS antenna. A weighted non-linear least squares solution is obtained for position estimation using trilateration, excluding these non line of sight satellites. Significant improvements in position estimation results, obtained from extensive experiments carried out in urban scenarios over a period of several weeks, validate the applicability and feasibility of the proposed method.

1 INTRODUCTION

Precise position estimation has always attracted key attention in intelligent transport systems primarily because it is a prerequisite for autonomous navigation and driver assistance services [1]. Driver assistance services such as lane change assistance, need an accurate position estimate of the vehicle for their operation and for driver safety. Global Navigation Satellite System (GNSS) is one of the most commonly used technologies for position estimation in urban scenarios. GNSS has advanced a lot since its inception in 1978 and present day technology is capable enough to precisely estimate the position anywhere on or above the surface of the earth within a few centimeters of accuracy [2]. With the advancement in satellite technology, highly

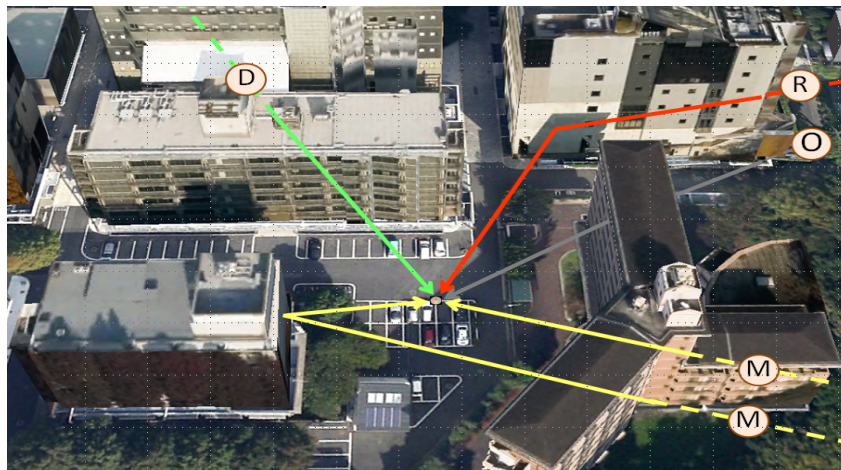


Figure 1: GPS signals received directly (green), with multipath (yellow) and after reflection (red)

sophisticated satellites have been launched into various constellations, viz. Global Positioning System (GPS) by the United States of America, and Global Orbiting Navigation Satellite System (GLONASS), by USSR [3]. More recently, Japan introduced a satellite augmentation system called quasi-Zenith Satellite System (QZSS). The advantage of QZSS for navigation in Japan is that its apogee is over Japan, and at least one satellite will always be visible with high elevation (*more than* 60°) at any point in Japan [4]. Because the signal format of QZSS is similar to that of GPS, conventional GPS receivers would be able to receive signals from QZSS [5]. In spite of such a wonderful technology, an issue still persists when position estimation needs to be done in urban scenarios where direct line of sight to GPS satellites is not that obvious because of the presence of canyons of tall buildings. QZSS can handle such a situation to some extent, but because of its initial phase and its availability only over Japan, more attention needs to be paid to overcome the occlusion of GPS satellites in urban scenarios. In an open space, satellites from which GPS signals are received, are likely to be in line of sight to the measurement point giving a position accuracy which is sufficient for many ITS applications [6].

However, position accuracy degrades drastically due to errors caused by multiple paths taken by GPS signals in urban scenarios [7]. Such errors are basically due to the following two reasons. The first reason for error is when multiple signals are received from a satellite: direct signals, as well as those reflected from the surrounding buildings (*M in Fig.1*). Such errors can be mitigated after considering the signal to noise ratio (SNR) of the received signal [8]. A second reason for error is the case when the signal is received only after reflections from the surrounding buildings, without receiving direct signal (*R in Fig.1*). This happens when a satellite is not in the line of sight with the GPS receiver. In the later case, the error magnitude might surge to several hundred meters especially in a case where surrounding structures have highly reflective surfaces [9]. Existing methods only detect multipath errors if the direct signal is also received along with the reflected signal. Such methods work either by considering signal-to-noise ratio (SNR) or by using interference patterns between a directly received signal and a signal received after reflections. Therefore, such methods can not detect a reflected signal if it is not accompanied by a directly received signal.

In this paper, we deal with the case where signals are received only after reflections, and exclude those signals from position estimation calculations. This is made feasible by making use of a 3D map of the environment around the measurement point using a laser range sensor. The rest of the paper is organized as follows. Related work is discussed in Section 2. We introduce the problem and describe our proposed solution in Section 3. Building a 3D map with laser scanner, and position estimation excluding non line of sight satellites, is discussed in Section 4. Experimental set-up and results are presented in Section 5. The conclusion of the work is presented in Section 6.

2 RELATED WORK

Reliable and precise position estimation has been attempted in the past by many researchers. Some of them use single position sensors while others rely on sensor fusion with multiple sensors. A sensor fusion based approach combining a GPS with an inertial measurement unit (IMU) and using an Extended Kalman Filter has been attempted in [10]. The method compensates for missing GPS positions with the help of the inertial measurement unit (IMU) however, direct attention to multipath has not been paid. An antenna array with a GPS software receiver has been used to detect the presence of multipath in [11]. Multipath contamination, with the assumption of a static surrounding environment, has been formulated as a regression problem in [12] in which multipath errors corresponding to a satellite are modeled using a training data as a

function of satellite geometry w.r.t. the receiver. The problem of ego-position for vehicles in dense urban areas is solved based on a ray tracing model in [13] in which a multi-constellation of satellites consisting of GPS and GLONASS systems has been used for precise positioning. An omni-directional IR camera has been used to capture sky region and the captured IR images are post processed and binarized to detect non line of sight satellites [14]. The method relies on publicly available datasets to estimate the height of buildings, however, such datasets become obsolete until a new dataset is reconstructed. The work done in [15] evaluates shadow maps of building models and uses that to estimate blocked reception conditions. The method might work fine on a fine sunny day, however it has obvious limitations on a cloudy day and would totally fail in the dark.

Our method considers a 3D geometric map of the surrounding environment, which is created at the time of the GPS measurement. The 3D map is built from range images in [16] and [17], however each of these methods suffers from high computation in the case of large scale modeling. We use a fast and simultaneous approach for range image alignment [18]. Using a 3D map at the time of GPS measurement has several advantages, one is that the map is always updated and secondly, it considers the dynamic occlusions which could occur due to parked vehicles or other reflective surfaces nearby at the time of measurement. To the best of the authors' knowledge, this is the first attempt where a highly precise 3D map of the environment is built and considered to identify satellites from which a signal is received after reflections.

3 PROBLEM STATEMENT AND APPROACH

Radio signal transmitted by a GPS satellite S_i contains information about its position P_i at the time of transmission (*known as time of ephemeris*) t_{oe} . A GPS receiver receives these signals and estimates its current position using trilateration. Trilateration is a technique to find the position of an unknown point by knowing its distance from a number of known points (*at least 3*). In GPS, this distance (*known as pseudo-range*) ρ is calculated by multiplying the time Δt which the signal took to reach the receiver traveling at the velocity of light ($c \simeq 2.9979 \times 10^8 \text{ m/s}$). Because the receiver clock is not synchronized with the satellite clock, an additional satellite is required to compensate for clock offset δt_{offset} . If the signal is received from more than 4 satellites, a least squares solution can be obtained for the position estimation. In the general case, measured pseudo-range ρ_m is larger than its true value ρ_0 because of many atmospheric factors. The error in pseudo-range due to atmospheric effects can be corrected using correction parameters which are embedded into the radio signal. However, apart from that, there are other disturbances which are not known at source side and depend purely on the environment around the receiver. These errors are due to the reflection of the signal before it reaches the GPS antenna. In the case of multipath, direct signals as well as signals after reflections are received by the receiver. Such multipath errors can either be eliminated using signal-to-noise ratio (SNR) or using interference patterns.

However, when the signal received from a satellite is only after reflection, without having received any direct signal, existing methods can not be used to correct for the pseudo-range. Hence, position estimates obtained from trilateration using erroneous pseudo-ranges are several hundred meters away from their true positions depending upon the severity of the signal reflections at that point. This will be demonstrated in section 5. To deal with the position errors due to signal reflections, we first identify the signals which are received after reflections using a 3D map of the environment, and then exclude those signals from the position calculation.

4 BUILDING 3D MAP AND POSITION ESTIMATION FROM LINE-IN-SIGHT SATELLITES ONLY

This section describes the method to find occlusion of satellites from the surrounding environment and the method to exclude the reflected signals from the position calculation.

4.1 CAPTURING 3D ENVIRONMENT WITH RANGE SCANS

A laser range scanner is used to scan the 3D environment around each measurement point. Each scan samples the surrounding geometry in 3D with a resolution specified by the user. The sampled points are obtained in a coordinate system with its center as center of scanner, which coincides with the point of GPS measurement. The scans at each measurement point are aligned into a common coordinate system using [18] which also corrects orientation. Fig. 2 shows a 3D range scan taken at the measurement point.

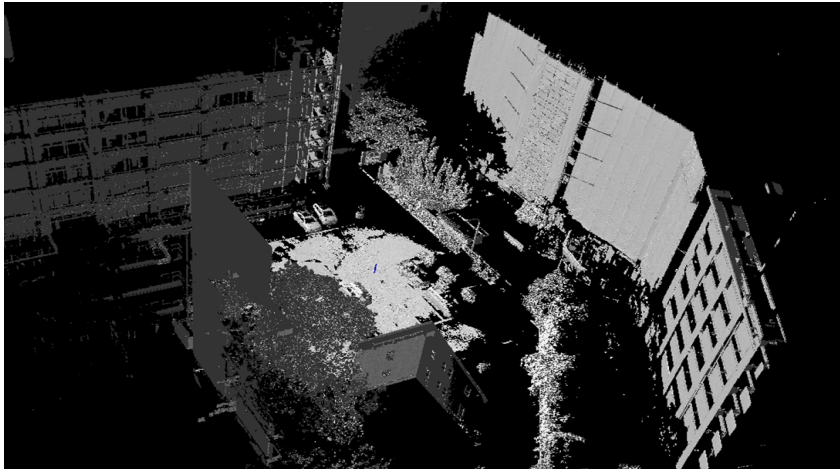


Figure 2: 3D range scan at measurement point

4.2 SATELLITE POSITION CALCULATION

Raw GPS measurements are converted into Receiver INdependent EXchange Format (RINEX) which outputs two types of messages. One is the *navigation message* containing orbital parameters of satellites and correction factors for atmospheric effects and satellite clock errors. The other message is the *observation message* which contains the pseudo-range of each satellite. The orbital positions x and y of the satellites, obtained after making corrections to various atmospheric effects and clock offsets, are converted into ECEF coordinates $P_i(X_i, Y_i, Z_i)$ as follows.

$$\begin{bmatrix} X_i \\ Y_i \\ Z_i \end{bmatrix} = \begin{bmatrix} \cos \Omega \cos \omega - \sin \Omega \sin \omega \cos i & -\cos \Omega \sin \omega - \sin \Omega \cos \omega \cos i & \sin \Omega \sin i \\ \sin \Omega \cos \omega + \cos \Omega \sin \omega \cos i & -\sin \Omega \sin \omega + \cos \Omega \cos \omega \cos i & -\cos \Omega \sin i \\ \sin \omega \sin i & \cos \omega \sin i & \cos i \end{bmatrix} \begin{bmatrix} x \\ y \\ 0 \end{bmatrix} \quad (1)$$

where i , ω and Ω are orbital inclination, argument of perigee, and longitude of ascending node of orbital plane respectively. The satellite positions in ECEF coordinates are shown in Fig. 3. To exclude pseudo-ranges of satellites from which the signal is received after reflections, we need to find the occlusion of satellites in the 3D range scan. To find such occlusions, satellites are projected on to a panoramic image rendered from a 3D scan. First, we calculate azimuthal angle θ_i and elevation angle ϕ_i of satellite S_i w.r.t. GPS antenna, and then project it on a rendered image to find occlusions. There are two options for this process. One is by capturing

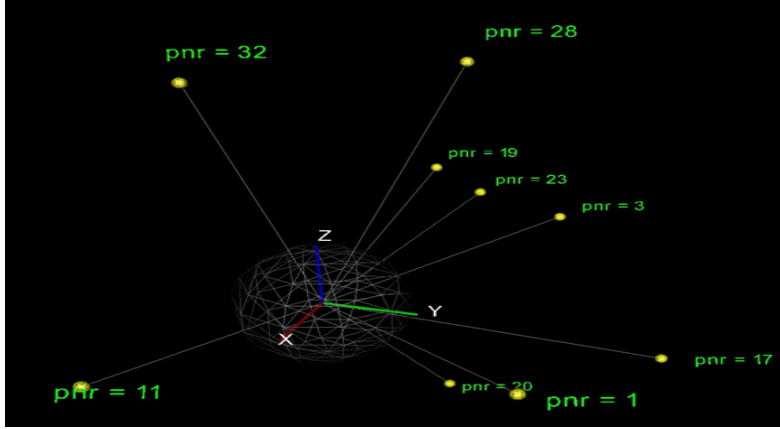


Figure 3: Satellite positions in ECEF coordinates

GSV sentence of NMEA format which gives azimuth θ_i and elevation ϕ_i of satellite S_i w.r.t. user antenna directly. Another is, obtaining satellite positions w.r.t. approximate user position obtained from raw GPS data, and then converting that data into spherical coordinates θ_i and ϕ_i as follows.

$$\begin{aligned} x_i &= r \sin \theta_i \cos \phi_i \\ y_i &= r \sin \theta_i \sin \phi_i \\ z_i &= r \cos \theta_i \end{aligned} \quad (2)$$

where (x_i, y_i, z_i) is the position of the satellite w.r.t. approx. user position and r is the distance of the satellite from the receiver. We use the first approach to find θ_i and ϕ_i .

4.3 POSITION ESTIMATION CONSIDERING SIGNAL CONDITIONS

In the case where satellite clocks and receiver clocks are synchronized, a *non-linear least-squares solution* can be obtained as follows.

$$\left[\hat{P}_{ant} \right] = \underset{P_{ant}}{\operatorname{argmin}} \sum_{i=1}^N \| P_i - P_{ant} \|^2 - \rho_i \quad (3)$$

where P_{ant} is position of GPS antenna and P_i is position of satellite. N is number of satellites from which signal is received and ρ_i is pseudo-range of satellite S_i . Because there is clock offset Δd_{offset} between the satellite clock and receiver clock, equation (3) is modified to equation (4).

$$\left[\hat{P}_{ant}, \Delta \hat{d}_{offset} \right] = \underset{P_{ant}, \Delta d_{offset}}{\operatorname{argmin}} \sum_{i=1}^N \| P_i - P_{ant} \|^2 - \rho_i + \Delta d_{offset} \quad (4)$$

However, equation (4) considers all satellites irrespective of whether or not they are in line of sight with the GPS antenna. To consider only line of sight satellites, we incorporate weights w_i in the optimization problem and solve it using *Levenberg-Marquardt algorithm* as in equation (5).

$$\left[\hat{P}_{ant}, \Delta \hat{d}_{offset} \right] = \underset{P_{ant}, \Delta d_{offset}}{\operatorname{argmin}} \sum_{i=1}^N w_i \left(\| P_i - P_{ant} \|^2 - \rho_i + \Delta d_{offset} \right) \quad (5)$$

The stopping criterion is set as in equation (6) below.

$$\frac{P_{ant}^{(k)} - P_{ant}^{(k+1)}}{P_{ant}^{(k)}} \leq 0.0001 \quad (6)$$

where $P_{ant}^{(i)}$ is antenna position obtained at i^{th} iteration. The algorithm is converged to optimal position P_{ant} which excludes reflected signals.

4.4 PROJECTION OF SATELLITES ON RENDERED IMAGES

The point cloud after alignment into common coordinate system are rendered into panoramic images $U(i, j)$. The satellites projected on to the rendered panoramic image are shown in Fig. 4. An azimuthal angle $\theta_i = 0^\circ$ and elevation angle $\phi_i = 0^\circ$ is fixed at the center $U(\frac{W}{2}, \frac{H}{2})$ of the panoramic image, where W and H are the horizontal and vertical resolution of the rendered image respectively.

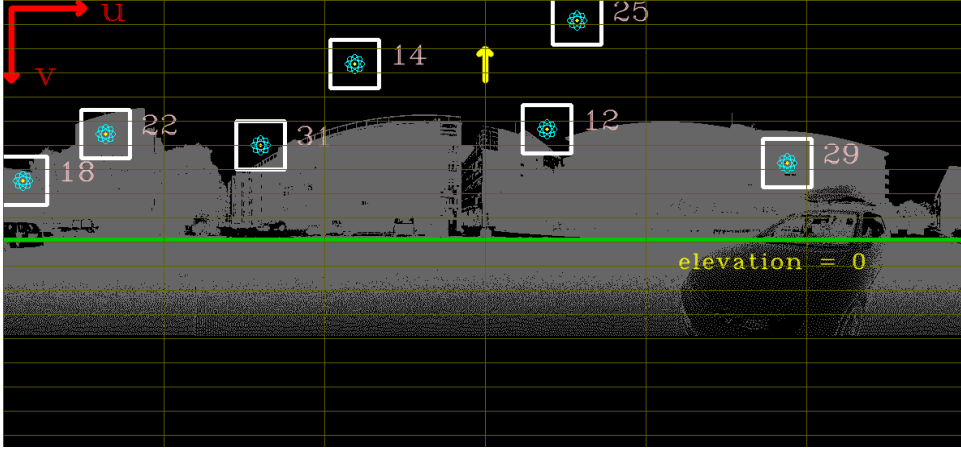


Figure 4: Finding satellite occlusions from rendered scan image

To find occlusion of satellites from the surrounding environment, a rectangular window $w(m, n)$ is placed with its center as the position of the satellite. Average pixel intensity in each window is calculated as follows:

$$I_{avg} = \frac{1}{m.n} \sum_{i=0}^m \sum_{j=0}^n U(i, j) \quad (7)$$

A binary weight w_i is assigned to each satellite based on if I_{avg} for satellite S_i is above or below a threshold I_{thresh} which is chosen empirically.

5 EXPERIMENTAL RESULTS AND DISCUSSION

5.1 EXPERIMENTAL SETUP

The experimental setup consists of a GPS antenna mounted on the top of a laser range sensor with fixed coordinate transformation between their centers. We used a Trimble 5700 GPS receiver with external Zephyr antenna to capture raw GPS measurements and Leica ScanStation C10 for capturing the 3D environment as point cloud. We consider two datasets (*dataset-I* and *dataset-II*) in our experiments, both in urban scenarios with a canyon of tall buildings. In *dataset-I*, there is good dilution of precision of satellites as the geometry of buildings around the

measurement point is scattered all around 360° where as in *dataset-II*, the dilution of precision of satellites is not that favorable because measurement points are confined to an area where a long narrow strip of sky is visible at all the measurement points. To validate the proposed approach, experiments were carried out at different times of the day and under different weather conditions.

5.2 POSITIONING RESULTS

This section gives positioning results of the experiments for *dataset-I* and *dataset-II*. Table 1 and Table 2 show the number of satellites along with PRN, and θ , ϕ angles of satellites at measurement position 1 of *dataset-I*, respectively.

Table 1: Available satellites at each epoch

Sr. No.	Epoch #	No. of Satellites	PRN of Satellites
1	p_1	5	12, 14, 22, 25, 31
2	p_2	5	12, 14, 22, 25, 31
3	p_3	5	12, 14, 22, 25, 31
4	p_4	6	12, 14, 22, 25, 29, 31
5	p_5	7	12, 14, 18, 22, 25, 29, 31
6	p_6	6	12, 14, 18, 22, 25, 31
7	p_7	6	12, 14, 22, 25, 29, 31
8	p_8	6	12, 14, 22, 25, 29, 31

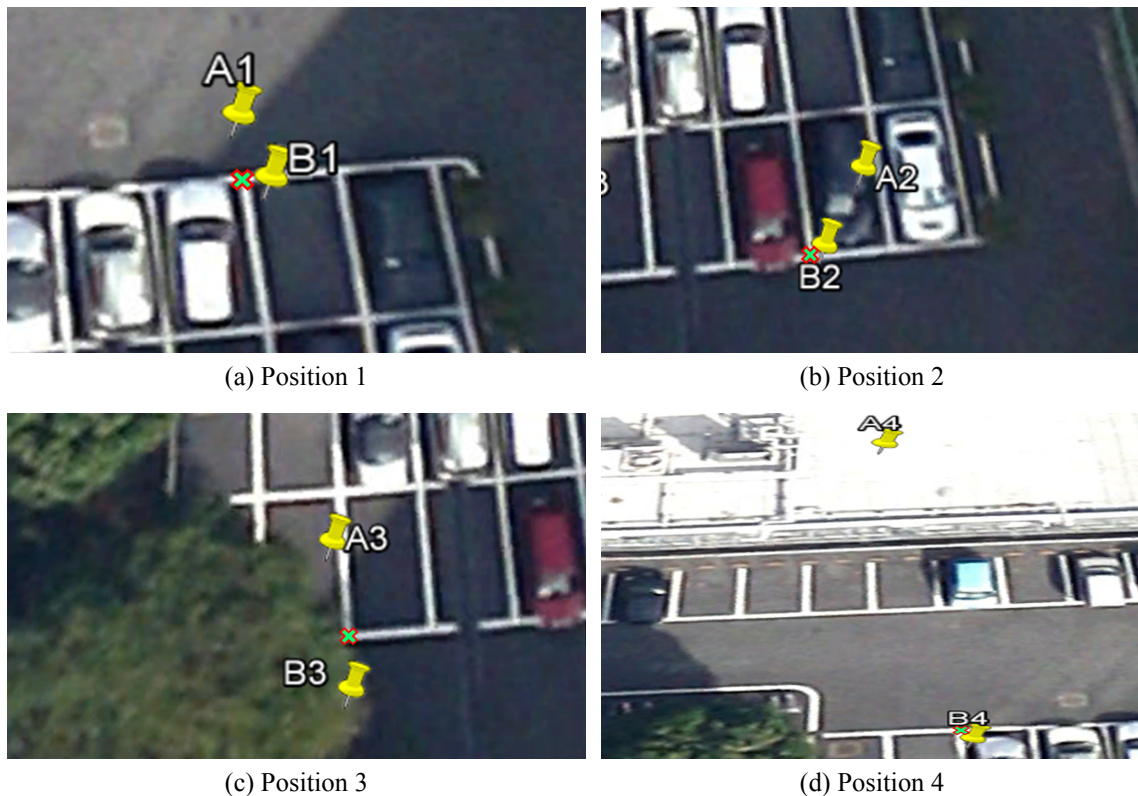


Figure 5: Observation (A), proposed method (B), ground truth (X) - DATASET-I

The estimated position from our method after removing occluded satellites using range data, and the positions directly given by the GPS receiver which considers only multipath errors using in-built circuitry, are shown in Fig. 5 and Fig. 6 for dataset-I and dataset-II respectively.

Position estimates obtained after exclusion of reflected signals are much more accurate than those obtained directly from the GPS receiver. It is mentioned here that ground truth points are marked manually on the aerial photographs.

Table 2: Satellite positions on rendered 3D scan

Sr. No.	PRN.	Elevation	Azimuth	u	v
1	12	37.9°	43.3°	670	186
2	14	64.3°	-35.4°	433	92
3	18	17.1°	-171.7°	24	261
4	22	35.9°	-137.9°	126	194
5	25	81.8°	55.9°	707	29
6	29	24.3°	142.1°	966	235
7	31	31.3°	-74.15°	317	210



Figure 6: Observation (A), proposed method (B), ground truth (X) - DATASET-II

5.3 PERFORMANCE COMPARISON AND DISCUSSION

To evaluate the performance of the proposed method, scatter of many observations taken at fix point is compared with and scatter of position estimates with proposed method. As a measure of scatter, a centroid is calculated from observations and mean square distance for each observation from the centroid is calculated. The Mean square distance is compared with that obtained from position estimates with proposed method. Two small datasets with few observation points taken near to the dataset whose 3D model has been built. Mean square error (*in meters*) of distance of each observation and position estimate obtained with proposed method from its corresponding centroid are shown in Table 3 and Table 4 for DATASET-I, and DATSET-II respectively.

Table 3: Mean Square Error of epochs from Centroid for DATASET-I

Sr. No.	Position #	MSE from centroid (without excluding reflected signals)	MSE from centroid (after excluding reflected signals)
1	P_1	3.4581	0.3005
2	P_2	5.4448	0.6501
3	P_3	6.2312	0.5854
4	P_4	1.0554	0.5933

It is observed that MSE calculated with proposed method is much smaller than that of direct observations. Furthermore, it is noticed that MSE after exclusion of reflected signals in DATASET-I is much smaller than that in DATASET-II. This is because dilution of precision is

more favorable in DATASET-I. Also, at epoch P_5 of DATASET-II, there is no change in MSE because the number of visible satellites is 4 and therefore no satellite was excluded. The MSE

Table 4: Mean Square Error of epochs from Centroid for DATASET-II

Sr. No.	Position #	MSE from centroid (without excluding reflected signals)	MSE from centroid (after excluding reflected signals)
1	P_1	14.8552	4.9845
2	P_2	15.1786	14.5083
3	P_3	5.0884	3.2900
4	P_4	4.5698	4.2792
5	P_5	0.8301	0.8301
6	P_6	3.6152	1.5189
7	P_7	14.7922	13.7926
8	P_8	12.6915	11.6046
9	P_9	11.2313	8.3656
10	P_{10}	5.5018	2.4111
11	P_{11}	0.7399	0.7028
12	P_{12}	0.7403	0.5704

of distance of position measurements from their centroids, with and without using the proposed method, clearly shows that with the proposed method, the measured points converge and the proposed method works effectively to improve the position estimation in urban scenarios.

5.4 MODELING RESULTS

A 3D model of huge building spread over 240m x 60m was built by taking a total of 149 partially overlapping scans using a laser range sensor. As each scan is in the local coordinate with its origin at the center of scanner, we aligned the scans into a common coordinate system using a fast simultaneous alignment method [18]. A 3D transformation between world positions obtained after exclusion of reflected signals and locally aligned scan centers was used to transform the locally aligned 3D model into world geodetic coordinates. The 3D model of DATASET-II in world geodetic coordinates is shown in Fig.7. The global positioning of the 3D model was verified by projecting a sparse set of points on aerial photographs.

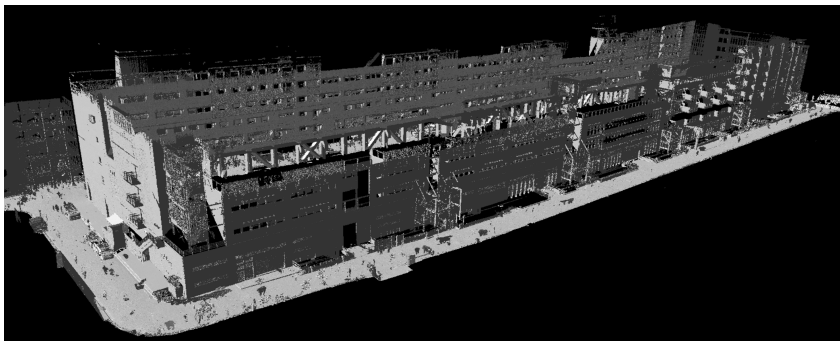


Figure 7: 3D model of urban structure in world geodetic coordinates

With the advancement of sensor technology, lightweight and inexpensive laser range sensors are available which can be mounted on the top of vehicles to find satellite reflections. Currently, GPS position estimation, using a GPS receiver, mounted on vehicles, which can not identify reflected GPS signals, results in large position estimation errors in urban scenarios. Using a laser range sensor on the top of the vehicle would improve the position estimation of vehicle by identifying and removing the reflected GPS signals.

6 CONCLUSION AND FUTURE SCOPE OF WORK

In this paper we have presented a method to improve position estimation in urban scenarios by identifying reflected GPS signals and excluding their pseudo-ranges from position calculation. A geometric 3D model is simultaneously built with laser range scanner to identify such reflected signals. Position estimates obtained considering only line of sight satellites shows a significant improvement in positioning than that obtained with multipath mitigation alone. A 3D model of a huge urban structure is built in world geodetic coordinates using the proposed method.

For future scope of the work, a low cost laser range scanner can be mounted on the top of the vehicle to scan the 3D environment in the form of sparse point cloud. Raw GPS measurements obtained with a GPS receiver can be used to find the satellite positions and their pseudo-ranges. The information from the GPS receiver and the laser scanner can be combined to exclude the reflected GPS signals as proposed in this method. Therefore, the precise GPS position estimates can be obtained for a vehicle driven in urban environments. Precise positioning of a vehicle would augment driving assistance services such as lane change assistance and collision avoidance for safety in intelligent transport systems.

ACKNOWLEDGEMENT

This work was supported, in part, by Next-generation Energies for Tohoku Recovery (NET) Project and by Strategic Information and Communications R&D Promotion Program (SCOPE) of Ministry of Internal Affairs and Communications, Japan.

References

- [1] Peter J. G. Teunissen, *A-PPP: Array-Aided Precise point Positioning With Global Navigation Satellite Systems*, IEEE Transactions on Signal Processing, Vol. 60, No. 6, June 2012.
- [2] Yaacob N, Abdullah M, Ismail M, *Multipath Mitigation of Global Positioning System (GPS) Signal Using Wavelet Technique*, IEEE International Conference on Digital Image Processing, Bangkok, March 2009.
- [3] Patrick Henkel, Christoph Gunther, *Precise point Positioning with multiple Galileo Frequencies*, IEE/ION Symposium on Position, Location and Navigation, Monterey, CA, May 2008.
- [4] Falin Wu, Nabuaki Kubo, Akio Yasuda, *Performance Evaluation of GPS Augmentation Using Quasi-Zenith Satellite System*, IEEE Transactions on Aerospace and Electronic Systems, vol. 40, No. 4, October, 2004.
- [5] Nabuaki Kubo, *How QZSS Contributes to Positioning Performance in Large Asian Cities?*, ICROS-SICE International Joint Conference, Fukuoka, Japan, August, 2009.
- [6] J. Sebastian Knogl, Patrick Henkel, and Christoph Gunther, *Precise Positioning and Orbit Estimation for Geostationary data Relays*, Proc. of 6th ESA Workshop on Satellite Navigation Technologies (NAVITEC), 2012.
- [7] Jimenez F, Naranjo J. E., Garcia F, Zato J G, Armingol J M, de la Escalera A, Aparicio, *Limitations of Positioning Systems for Developing Digital Maps and Locating Vehicles According to the Specifications of Future Driver Assistance Systems*, IET Intelligent Transport Systems, Issue 1, vol. 5, March 2011.
- [8] Pinchin J, Hide, C, Park D, Xiaoqi Chen, *Precise kinematic positioning using single frequency GPS receivers and an integer ambiguity constraint*, IEE/ION Symposium on Position, Location and Navigation, Monterey, CA, 2008.
- [9] Zavorotny V. U, Larson K. M, Braun J. J, Small E. E, Gutmann E. D, Bilich A. L, *A Physical Model for GPS Multipath Caused by Land Reflections: Toward Bare Soil Moisture Retrievals*, IEEE Journal of Selected Topics in Applied Earth Observations and Remote Sensing, Vol. 3, Issue 1, March 2010.
- [10] S. Panzieri, F. Pascuccit, G Ulivi, *An Outdoor Navigation System Using GPS and Inertial Platform*, in Proc. of IEEE/ASME International Conference on Advanced Intelligent Mechatronics, vol. 2, 2001.
- [11] M. T. Brenneman, Y.T. Morton, and Q. Zhou, *An ANOVA-Based GPS Multipath Detection Algorithm Using Multi-Channel Software Receivers*, in Proc. Joint IEEE PLANS and ION Annual Meeting, May 2008.
- [12] Quoc-Huy Phan, Su-Lim Tan, Ian McLoughlin, *GPS Multipath Mitigation: A Non-linear Regression Approach*, GPS Solut, Springer-Verlag, 2012.
- [13] Marcus Obst, Sven Bauer and Gerd Wanielik, *Urban Multipath Detection and Mitigation with Dynamic 3D Maps for Reliable Land Vehicle Localization*, in Proc. of IEEE/ION PLANS, 2012.
- [14] Jun-ichi Meguro, Taishi Murata, Jun-ichi Takiguchi, Yoshiharu Amano, and Takumi Hashizume, *GPS Multipath Mitigation for Urban Area Using Omnidirectional Infrared Camera*, IEEE Transactions on Intelligent Transport Systems, Vol. 10, No. 1, March 2009.
- [15] Sven Bauer, Marcus Obst, Robin Streiter and Gerd Wanielik, *Evaluation of Shadow Maps for Non-Line-of-Sight Detection in Urban GNSS Vehicle Localization with VANETS - The GAIN Approach*, Proc. of IEEE Intl. Conf. on IEEE 77th Vehicular Technology Conference: VTC2013-Spring, 2013.
- [16] P. Payeur, *3D modeling from range images with integrated registration*, IEEE International Workshop on Haptic Virtual Environments and Their Applications, 2002.
- [17] H. Hugli, T. Jost, *A match and merge method for 3D modeling from range images*, 6th International Conference on Signal Processing, 26-30 Aug. 2002.
- [18] T. Oishi, A. Nakazawa, R. Kurazume, and K. Ikeuchi, *Fast Simultaneous Alignment of Multiple Range Images Using Index Images*, Proc. of 5th International Conference on 3-D Digital Imaging and Modeling (3DIM), 2005.